INTRODUCTION TO INSERTION DEVICES

K. Wille
University of Dortmund, Germany

Abstract
Synchrotron radiation with extremely high brilliance is emitted by wiggler and undulator magnets, so called "insertion devices". They produce a periodically alternating field at the beam axis with well defined period length. The relativistic electron motion through the magnet is calculated. Because of the periodic transverse particle oscillation the resulting spontaneous radiation is mainly coherent with small width of spectral lines.

1. INTRODUCTION

At the very beginning the synchrotron radiation emitted by an electron beam passing through a bending magnet has been used for experiments. It is spread out over a wide horizontal fan as shown in Fig. 1. Since the probes are normally small, only a small fraction of the radiation is usable. Most of it is lost. In addition, the horizontal resolution is rather poor.

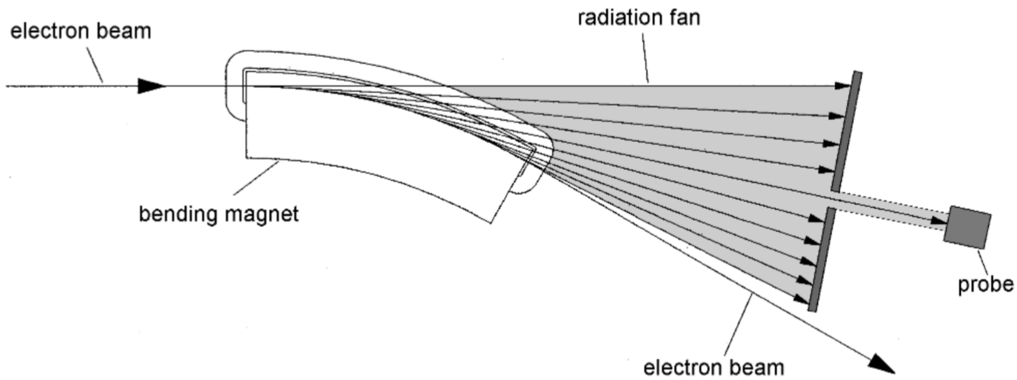

Fig. 1 Synchrotron radiation emitted by a bending magnet

Much better beam quality and significantly higher brilliance is provided by wiggler and undulator magnets (W/U magnets) [1] installed in special straight sections in electron storage rings. These types of magnets often are summarized under the name "insertion devices". The general arrangement of such magnets is sketched in Fig. 2. It consists of a sequence of short bending magnets of constant length. Along the beam axis the resulting field can be described in good approximation by a sine curve with the period length λ_u. The overall bending angle of this device vanishes. Therefore, sufficiently long straight sections are required in modern storage rings for synchrotron radiation to install the W/U magnets.

The design principal of wiggler magnets is basically the same as of undulator magnets. The difference comes from the field strength. Wigglers provide a strong field resulting in a wide horizontal opening angle of the emitted radiation. The wide photon spectrum is very similar to that of a bending magnet. The opposite are undulators with rather weak fields and correspondingly small opening angles of synchrotron light. In this case the photons can interfere and the emitted radiation is mainly coherent with a wavelength determined by the period length of the undulator and the beam energy. The intensity of this coherent radiation is by orders of magnitude higher than achieved from simple bending magnets.

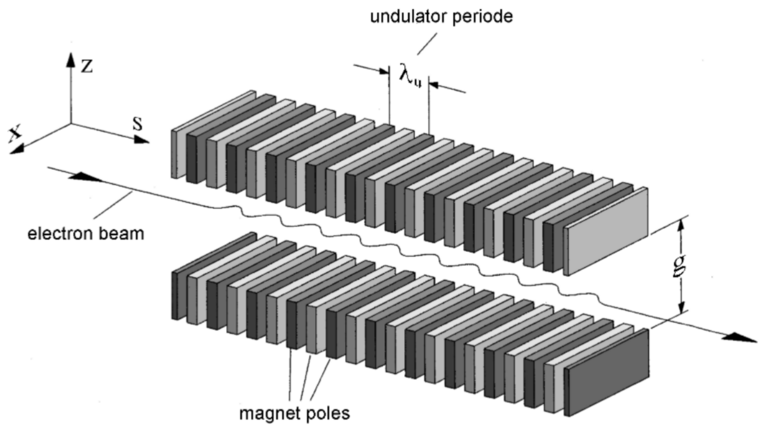

Fig. 2 General layout of a wiggler or undulator magnet

The synchrotron radiation from electron storage rings of the 3rd generation is essentially produced by wiggler and undulator magnets. A larger number of straight sections provide sufficient space for the insertion devices. The bending magnets only guide the beam along the circular orbit. The general layout of a modern synchrotron light source is sketched in Fig. 3. Some examples of third generation machines are listed in Table 1. More detailed informations are presented in [2].

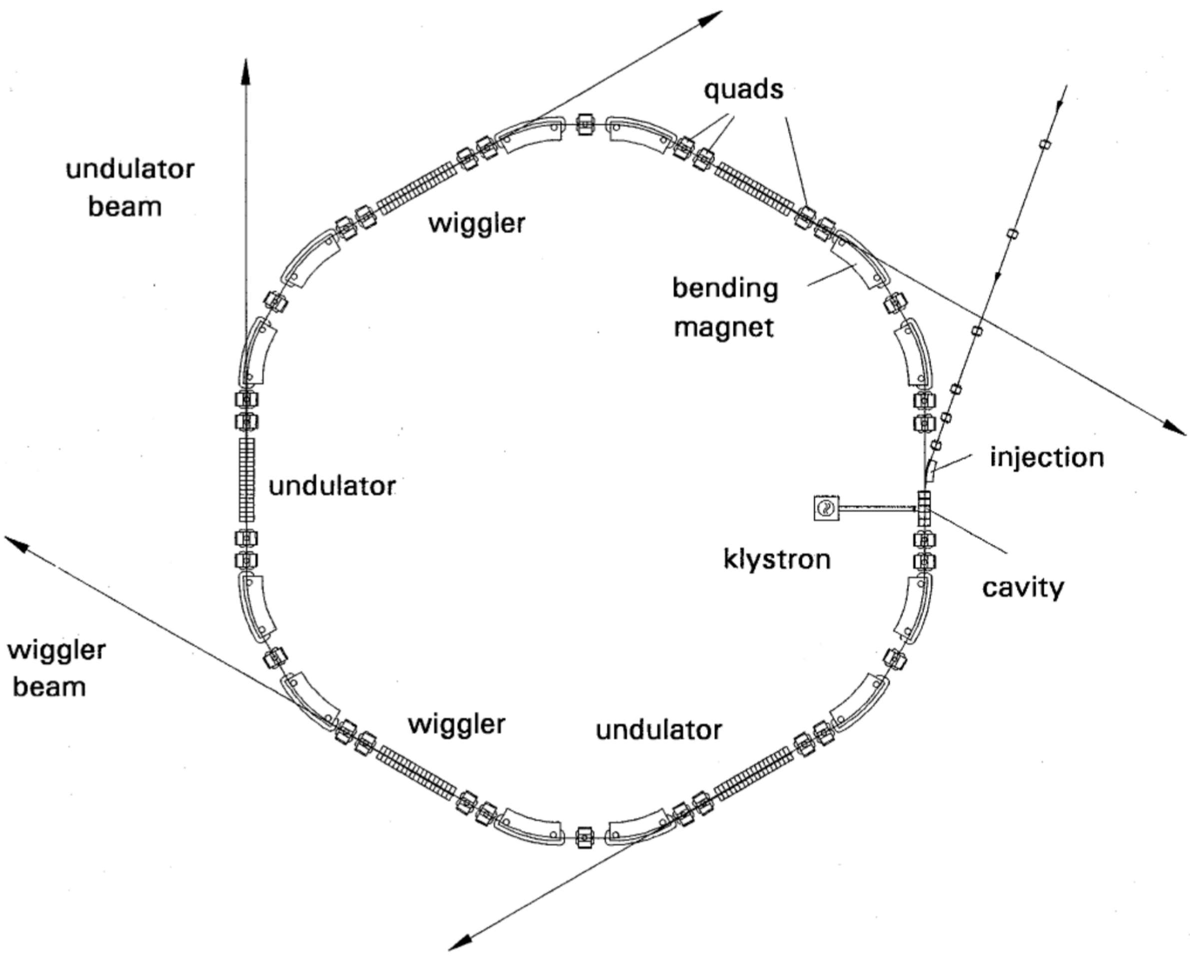

Fig. 3 General layout of a modern synchrotron light source of the 3rd generation

Table 1
List of some typical synchrotron light sources with insertion devices

Location	Ring	Energy [GeV]
Grenoble, France	ESRF	6.0
Argonne, USA	APS	7.0
Berkeley, USA	ALS	1.5
Trieste, Italy	ELETTRA	1.5 - 2.0
Dortmund, Germany	DELTA	1.5
Berlin, Germany	BESSY II	1.5 - 2.0

2. WIGGLER AND UNDULATOR FIELD

Wiggler and undulator magnets (W/U-magnets) produce in good approximation along the beam axis a periodic field with the scalar potential

$$\varphi(s,z) = f(z)\cos\left(2\pi\frac{s}{\lambda_u}\right) = f(z)\cos(k_u s). \tag{1}$$

Here a scalar potential is applied rather than a vector potential since in the interesting area around the beam no electrical current occurs. According to Fig. 2 s is the coordinate along the beam axis and z in the vertical direction. It is assumed that the magnet is unlimited in the horizontal (x coordinate) direction, providing a constant magnetic field along this coordinate. The vertical function $f(z)$ can be evaluated using Laplace equation

$$\nabla^2\varphi(s,z) = 0. \tag{2}$$

Taking (1) gives

$$\frac{d^2 f(z)}{dz^2} - f(z)k_u^2 = 0 \tag{3}$$

with the solution

$$f(z) = A\sinh(k_u z). \tag{4}$$

Substitution of (4) into the potential equation (1) yields

$$\varphi(s,z) = A\sinh(k_u z)\cos(k_u s). \tag{5}$$

For the particle motion inside a W/U-magnet only the vertical field is important. We can derive it simply from the potential by

$$B_z(s,z) = \frac{\partial\varphi(s,z)}{\partial z} = k_u A\cosh(k_u z)\cos(k_u s). \tag{6}$$

The unknown constant A can be estimated with an acceptable accuracy applying the strength of the poletip field B_0 as defined in Fig. 4.

According to equation (6) the poletip field at $z = g/2$ (g = gap height) is

$$B_0 = B_z\left(0,\frac{g}{2}\right) = k_u A\cosh\left(k_u\frac{g}{2}\right) = k_u A\cosh\left(\pi\frac{g}{\lambda_u}\right) \tag{7}$$

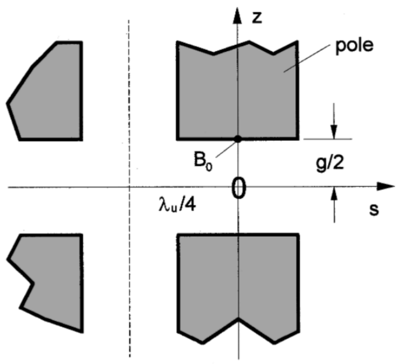

Fig. 4 Definition of the poletip field in a W/U-magnet

and the constant *A* becomes

$$A = \frac{B_0}{k_u \cosh\left(\pi \dfrac{g}{\lambda_u}\right)} . \tag{8}$$

With this result the W/U-field around the electron beam can finally be written in the form

$$B_z(s,z) = \tilde{B} \cosh(k_u z) \cos(k_u s) \tag{9}$$

with the peak field at the beam axis

$$\tilde{B} = \frac{B_0}{\cosh\left(\pi \dfrac{g}{\lambda_u}\right)} . \tag{10}$$

From this expression one can see that the peak field decreases very rapidly with increasing gap height *g*. This effect is also shown in Fig. 5.

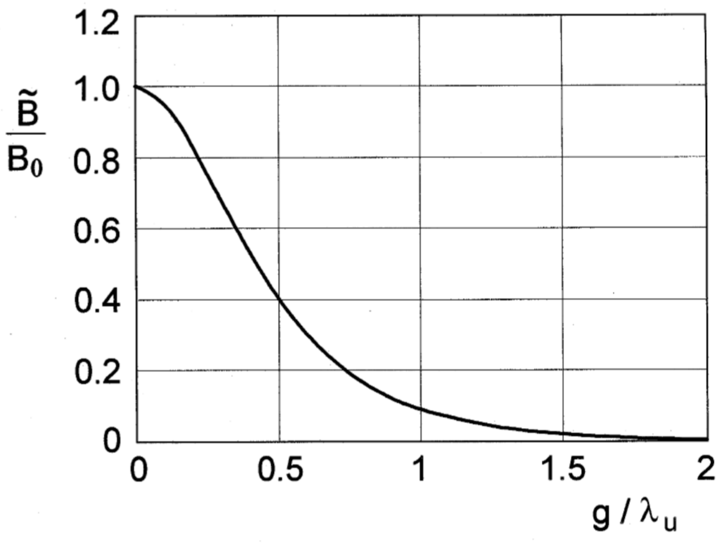

Fig. 5 Relative peak field at the beam axis as a function of the ratio g/λ_u

As a consequence of this behavior the gap height of a W/U-magnet has to be substantially smaller than the period length λ_u. This leads to very small gaps if short W/U-periods are required. The field calculation presented here is only a simple analytic approximation, it is helpful for basic investigations. For an accurate design including tight tolerances more sophisticated methods and numerical calculations are required [1, 3, 4].

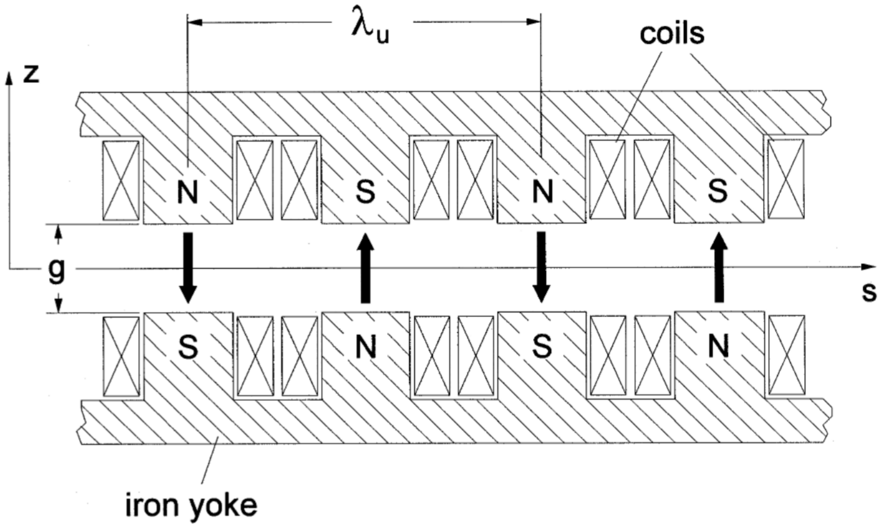

Fig. 6 Principal design of an electromagnetic wiggler or undulator

The very first W/U-magnets have been built with conventional iron yokes excited by magnet coils as shown in Fig. 6. The field strength can easily be changed by changing the current. This technique is used for period lengths not smaller than $\lambda_u \approx 25$ cm. For smaller periods the current density in the coils exceeds reasonable values. In this case one can take superconductive coils, but because of the cryostat and the expensive liquid helium technique the costs are disproportionate.

Therefore, another type of W/U-magnets has been developed utilizing small pieces of permanent magnets arranged as sketched in Fig. 7.

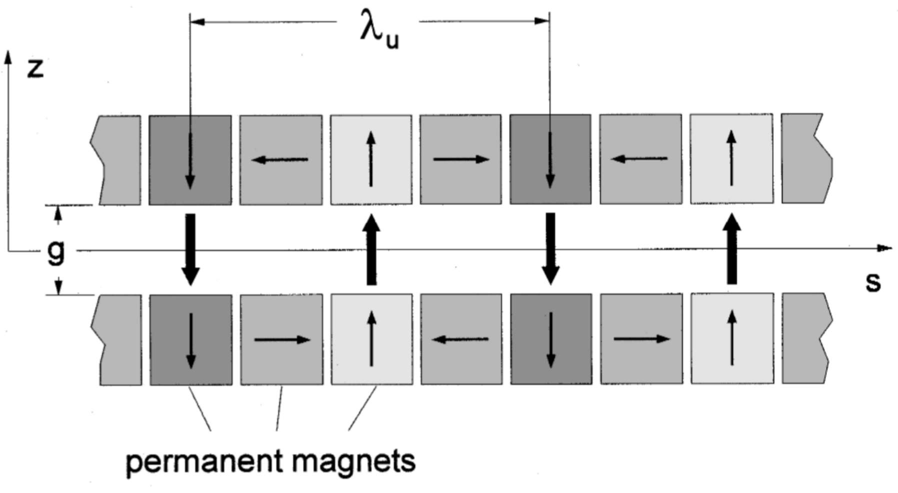

Fig. 7 W/U-magnet built with permanent magnets. The arrows indicate the orientation of the magnetic flux.

Since the flux density in the magnet pieces is constant, one can only vary the field strength at the beam axis by opening or closing the gap mechanically. The field changes according to equation (10). The poletip field has values which depend on the material used. For instance, samarium-cobalt ($SmCo_5$) provides flux densities about $B \approx 0.9$ - 1.0 T. If higher fields up to 2 T are required, one can built hybrid magnets (Fig. 8). They consist of poles made by soft iron and pieces of permanent magnets in between. The total flux of the magnet pieces is concentrated in the iron poles resulting in poletip fields about $B_0 = 2$ T.

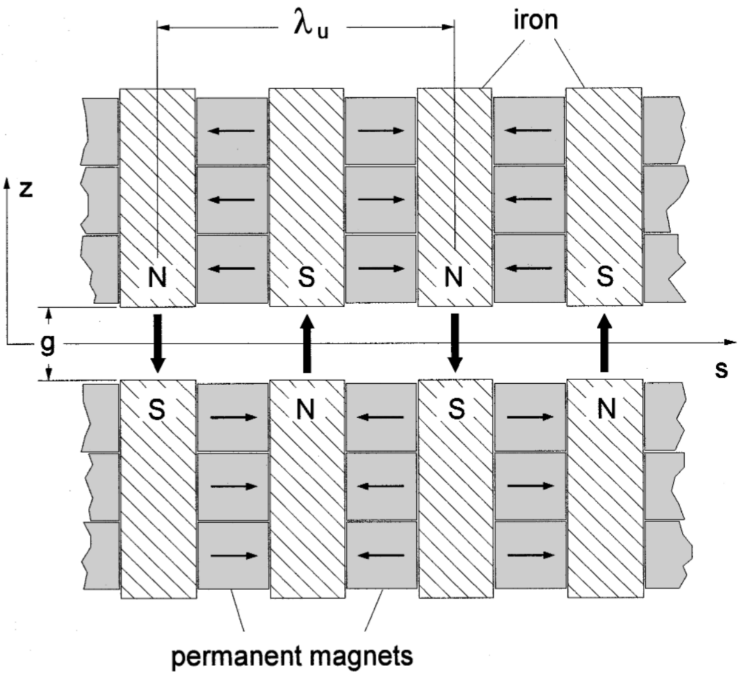

Fig. 8 Sketch of a hybrid magnet with iron poles exited by permanent magnet pieces

As mentioned above, the W/U-magnets are installed in straight sections of the storage ring. Thus, the total bending angle of the entire device must vanish (Fig. 9).

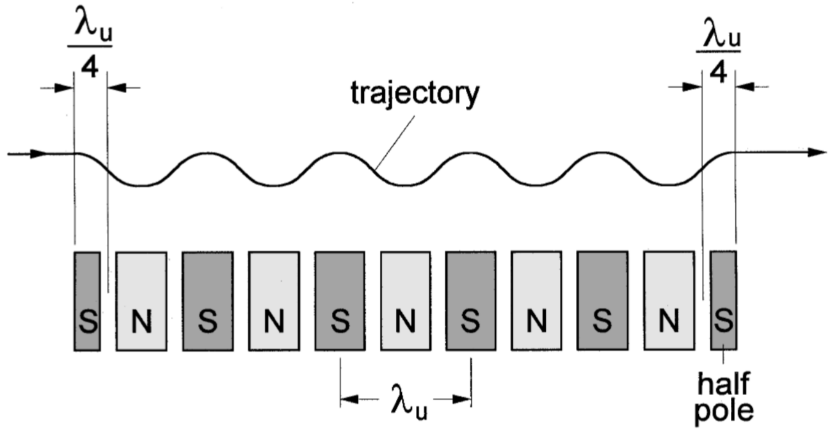

Fig. 9 Matching condition for the beam orbit over a W/U-magnet

This leads directly to the following matching condition:

$$\int_{\mathrm{W/U}} B_z(s)\,ds = \tilde{B}\int_{s_1}^{s_2}\cos(k_u s)\,ds = 0\,. \qquad (11)$$

It is satisfied if

$$s_1 = 0 \qquad \text{and} \qquad s_2 = n\lambda_u + \frac{\lambda_u}{2} \quad (n = 1,2,\ldots) \qquad (12)$$

Very often this condition is realized by adding a magnet pole of half the length of a normal pole at the entrance and the exit of the magnet. The beam oscillation is then asymmetric with respect to the beam axis (Fig. 9). If symmetric oscillation is required, i.e. for free electron lasers, more sophisticated conditions can be applied.

3. EQUATION OF MOTION IN W/U-MAGNETS

3.1 The coupled set of equations of motion

Inside a W/U-magnet with the field $\boldsymbol{B}$ the Lorentz force

$$\boldsymbol{F} = \dot{\boldsymbol{p}} = m\gamma\,\dot{\boldsymbol{v}} = e\,\boldsymbol{v}\times\boldsymbol{B} \tag{13}$$

acts on the relativistic electron with the mass $m\gamma$ and the charge e. In the following we will only discuss the particle motion in the horizontal x-s-plane. The vertical motion is normally negligible. With this simplification we can write the field of the W/U-magnet and the particle velocity $\boldsymbol{v}$ in the form

$$\boldsymbol{B} = \begin{pmatrix} 0 \\ B_z \\ B_s \end{pmatrix} \qquad \text{and} \qquad \boldsymbol{v} = \begin{pmatrix} v_x \\ 0 \\ v_s \end{pmatrix}. \tag{14}$$

Inserting (14) into (13) directly provides

$$\dot{\boldsymbol{v}} = \frac{e}{m\gamma}\begin{pmatrix} -v_s B_z \\ -v_x B_s \\ v_x B_z \end{pmatrix}. \tag{15}$$

We again neglect the vertical particle motion and can finally write the result in the form of a coupled set of equations:

$$\boxed{\begin{aligned} \ddot{x} &= -\dot{s}\frac{e}{m\gamma}B_z(s) \\ \ddot{s} &= \dot{x}\frac{e}{m\gamma}B_z(s) \end{aligned}} \tag{16}$$

3.2 First-order solution of the equations of motion

Since $B_z(s)$ is a nonlinear function of the position s in the magnet (see eq. (9)), there exists no simple analytic solution. The longitudinal velocity v_s, however, is significantly larger than the horizontal component v_x. This fact allows us to write

$$\dot{x} = v_x << v_s \qquad \text{and} \qquad \dot{s} = v_s = \beta c = \text{const.} \tag{17}$$

Under these conditions, only the first equation of (16) is of interest and we get the relation

$$\ddot{x} = -\dot{s}\frac{e}{m\gamma}B_z(s) = -\frac{\beta c e\tilde{B}}{m\gamma}\cos(k_u s). \tag{18}$$

In storage rings it is often more convenient to describe the particle motion as a function of place s instead of time t. For transformation we use

$$\dot{x} = x'\beta c \qquad \text{and} \qquad \ddot{x} = x''\beta^2 c^2 \tag{19}$$

and get from equation (18) the first order expression of the particle motion

$$x'' = -\frac{e\tilde{B}}{m\beta c\gamma}\cos(k_u s) = -\frac{e\tilde{B}}{m\beta c\gamma}\cos\left(2\pi\frac{s}{\lambda_u}\right). \tag{20}$$

It can be easily solved by integration. Since the electrons in storage rings for synchrotron radiation have extremely relativistic velocities, we can set $\beta = 1$ and obtain

$$
\begin{aligned}
x'(s) &= \frac{\lambda_u e \tilde{B}}{2\pi m\gamma c} \sin(k_u s) \\
x(s) &= \frac{\lambda_u^2 e \tilde{B}}{4\pi^2 m\gamma c} \cos(k_u s).
\end{aligned}
\tag{21}
$$

The first equation gives the angle of the particle trajectory in a W/U-magnet with respect to the orbit (Fig. 10).

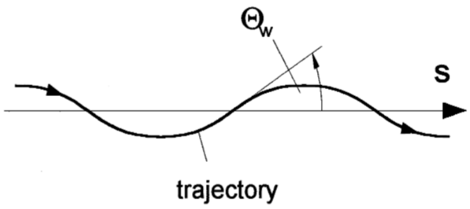

Fig. 10 Particle trajectory in a W/U-magnet

The maximum value of the trajectory angle is achieved at the crossing points with the orbit. It is

$$
x'_{\max} = \Theta_w = \frac{1}{\gamma} \frac{\lambda_u e \tilde{B}}{2\pi mc}. \tag{22}
$$

Now we define the dimensionless **wiggler** or **undulator parameter**

$$
\boxed{K = \frac{\lambda_u e \tilde{B}}{2\pi mc}} \tag{23}
$$

and can write the maximum trajectory angle in the form

$$
\Theta_w = \frac{K}{\gamma}. \tag{24}
$$

Especially for $K = 1$ the angle becomes

$$
\Theta_w = \frac{1}{\gamma}, \tag{25}
$$

which is identical to the natural opening angle of the synchrotron radiation cone. This relation suggests now the following differentiation between wiggler and undulator magnets:

$$
\boxed{\begin{array}{llll}
\text{Undulator} & \text{if} & K \le 1 & \text{i.e.}\quad \Theta_w \le \dfrac{1}{\gamma} \\
\text{Wiggler} & \text{if} & K > 1 & \text{i.e.}\quad \Theta_w > \dfrac{1}{\gamma}
\end{array}} \tag{26}
$$

For very large K the horizontal opening angle of the radiation is correspondingly large and no interference of the photons takes place. The photon energy covers a dipole-like broad spectrum. For very small K the radiation from all undulator periods overlaps and strong interference effects occur, resulting in rather sharp coherent spectral lines.

3.3 Second-order solution of the equations of motion

With the simple first-order solution we can't describe for instance the Doppler effect observed in wiggler and undulator radiation. Therefore, we have to take additional conditions into account. But we are still not going to look for a general solution of the coupled set of equations of motions (16).

The longitudinal velocity $\dot{s}$ causes, because of the Lorentz force, a transverse oscillation $x(t)$, as described by equation (21). The resulting transverse velocity again causes a small longitudinal oscillation, which superimposes with the longitudinal velocity $\dot{s}$. The longitudinal velocity is actually not really constant. Thus, we can describe the particle motion in the form

$$\dot{s}(t) = \langle \dot{s} \rangle + \Delta \dot{s}(t) \tag{27}$$

with the average velocity $\langle \dot{s} \rangle$ and the longitudinal oscillation $\Delta \dot{s}(s)$. As shown in Fig. 11 the constant particle velocity βc can be written as

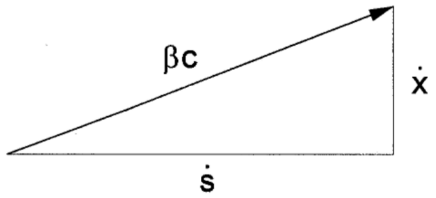

Fig. 11 Addition of the particle velocity

$$(\beta c)^2 = \dot{s}^2 + \dot{x}^2 . \tag{28}$$

With

$$\beta^2 = 1 - \frac{1}{\gamma^2} \tag{29}$$

we find

$$\dot{s}(t) = c\sqrt{1 - \left(\frac{1}{\gamma^2} + \frac{\dot{x}^2}{c^2}\right)} . \tag{30}$$

Since $1/\gamma^2 << 1$ and $\dot{x} << c$ we can expand the root. The longitudinal has therefore the expression

$$\dot{s}(t) = c\left[1 - \frac{1}{2}\left(\frac{1}{\gamma^2} + \frac{\dot{x}^2(t)}{c^2}\right)\right] = c\left[1 - \frac{1}{2\gamma^2}\left(1 + \frac{\gamma^2}{c^2}\dot{x}^2(t)\right)\right]. \tag{31}$$

Taking the formula (21) and (23) gives

$$x'(s) = \frac{K}{\gamma}\sin(k_u s) . \tag{32}$$

With the transformations

$$\dot{x} = \beta c x', \quad s = \beta c t \quad \text{and} \quad \omega_u = k_u \beta c \tag{33}$$

we get the time-dependent transverse velocity

$$\dot{x}(t) = \beta c \frac{K}{\gamma} \sin(\omega_u t)\,. \tag{34}$$

We insert this relation into equation (31) and convert the sine function according to

$$\sin^2(x) = \frac{1}{2}\left(1 - \cos(2x)\right). \tag{35}$$

The longitudinal velocity becomes

$$\dot{s}(t) = c\left\{1 - \frac{1}{2\gamma^2}\left[1 + \frac{\beta^2 K^2}{2}\left(1 - \cos(2\omega_u t)\right)\right]\right\}. \tag{36}$$

It has the required form of equation (27) with the average velocity

$$\langle \dot{s} \rangle = c\left\{1 - \frac{1}{2\gamma^2}\left[1 + \frac{\beta^2 K^2}{2}\right]\right\} \tag{37}$$

and the time-dependent velocity oscillation

$$\Delta\, \dot{s}(t) = \frac{c\,\beta^2 K^2}{4\gamma^2} \cos(2\omega_u t)\,. \tag{38}$$

For extremely relativistic particles we set $\beta = 1$. This condition is fulfilled in almost all storage rings for synchrotron radiation. The relative velocity of the particle along the undulator axis is

$$\beta^* = \frac{\langle \dot{s} \rangle}{c} = 1 - \frac{1}{2\gamma^2}\left[1 + \frac{K^2}{2}\right]. \tag{39}$$

Thus, we can write the transverse and longitudinal particle velocity in the form

$$\begin{aligned} \dot{x}(t) &= \frac{cK}{\gamma} \sin(\omega_u t) \\ \dot{s}(t) &= \beta^* c + \frac{cK^2}{4\gamma^2} \cos(2\omega_u t). \end{aligned} \tag{40}$$

The trajectory can finally be found simply by integrating these equations using the arbitrary initial conditions $x(0) = 0$ and $s(0) = 0$:

$$\begin{aligned} x(t) &= -\frac{K}{k_u \gamma} \cos(\omega_u t) \\ s(t) &= \beta^* ct + \frac{K^2}{8 k_u \gamma^2} \sin(2\omega_u t). \end{aligned} \tag{41}$$

It is very impressive to observe the particle motion in the coordinate system $\boldsymbol{K}^*$, which travels along the undulator axis with the constant velocity β^*, rather than in the laboratory system $\boldsymbol{K}$. With the Lorentz transformations

$$x^* = x \quad \text{and} \quad s^* = \gamma(s - \beta\, t) \tag{42}$$

we find the trajectory functions in the moving system $\boldsymbol{K}^*$

$$\boxed{\begin{aligned} x^*(t) &= -\frac{K}{k_u\gamma}\cos(\omega_u t) \\ s^*(t) &= \frac{K^2}{8k_u\gamma^2}\sin(2\omega_u t). \end{aligned}} \tag{43}$$

In this system the trajectory has a shape like an "8" as shown in Fig. 12. For very small values of the undulator parameter K only the transverse motion dominates. The "8" is very narrow. For larger K the longitudinal amplitude grows quadratically, whereas the transverse amplitude is proportional to K. The growing longitudinal motion causes a Doppler effect of the emitted radiation.

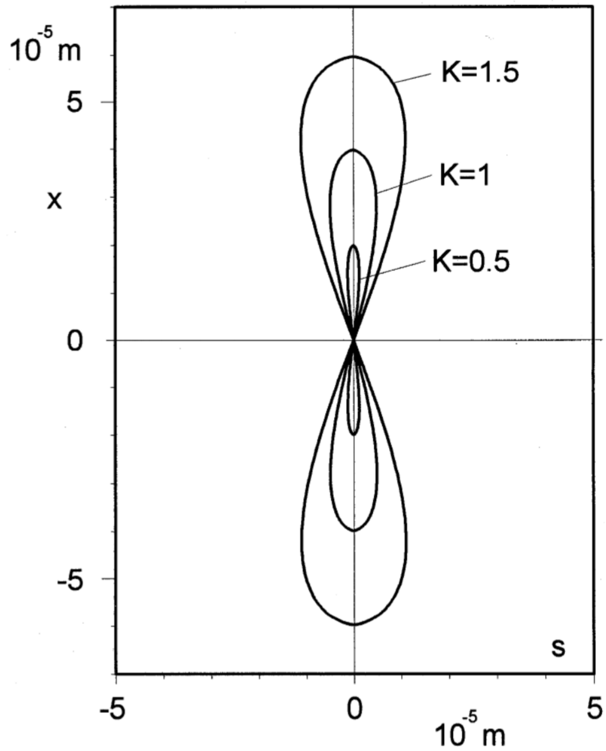

Fig. 12 Particle trajectory in an undulator magnet observed in the moving system $\boldsymbol{K}^*$

4. UNDULATOR RADIATION

The sinusodial particle motion in an undulator causes coherent radiation in the laboratory system $\boldsymbol{K}$ with the frequency

$$\Omega_{rad} = \frac{2\pi\beta c}{\lambda_u} = k_u\beta c\,. \tag{44}$$

For very small undulator parameters $K << 1$ we can neglect the longitudinal oscillation $\Delta\,\dot{s}(t)$ and find in the moving system $\boldsymbol{K}^*$ the monochromatic radiation with the frequency

$$\omega^*_{rad} = \gamma^*\Omega_{rad}\,. \tag{45}$$

γ^* is the relative energy of the particle in $\boldsymbol{K}^*$. We transform this radiation from the moving system into the laboratory system. Here, we take a photon with the momentum p emitted under the angle Θ_0 with respect to the undulator axis (Fig. 13).

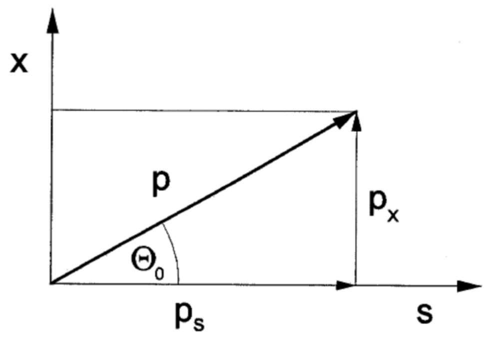

Fig. 13 Photon with the momentum p emitted in the laboratory system

The energy and the momentum of the photon are

$$E = \hbar\omega \qquad \text{and} \qquad p = \frac{\hbar\omega}{c} \tag{46}$$

and the 4-momentum becomes

$$P_\mu = \begin{pmatrix} E/c \\ p_x \\ p_z \\ p_s \end{pmatrix} = \begin{pmatrix} E/c \\ p\sin\Theta_0 \\ 0 \\ p\cos\Theta_0 \end{pmatrix}. \tag{47}$$

The transformation into the moving system $\boldsymbol{K}^*$ yields

$$\begin{pmatrix} E^*/c \\ p_x^* \\ p_z^* \\ p_s^* \end{pmatrix} = \begin{pmatrix} \gamma^* & 0 & 0 & -\beta^*\gamma^* \\ 0 & 1 & 0 & 0 \\ 0 & 0 & 1 & 0 \\ -\beta^*\gamma^* & 0 & 0 & \gamma^* \end{pmatrix} \cdot \begin{pmatrix} E/c \\ p\sin\Theta_0 \\ 0 \\ p\cos\Theta_0 \end{pmatrix}. \tag{48}$$

Considering equation (46), the resulting photon energy becomes

$$\frac{E^*}{c} = \gamma^* \frac{E}{c} - \beta^*\gamma^* p\cos\Theta_0 = \gamma^* \frac{\hbar\omega_{rad}}{c}\left(1-\beta^*\cos\Theta_0\right). \tag{49}$$

With $E^* = \hbar\,\omega^*_{rad}$ we get

$$\frac{\hbar\omega^*_{rad}}{c} = \gamma^* \frac{\hbar\omega_{rad}}{c}\left(1-\beta^*\cos\Theta_0\right). \tag{50}$$

From this equation we directly derive the frequency transformation of the relativistic Doppler effect

$$\omega_{rad} = \frac{\omega^*_{rad}}{\gamma^*\left(1-\beta^*\cos\Theta_0\right)}. \tag{51}$$

Using equations (44) and (45) we have

$$\omega_{rad} = \frac{\Omega_{rad}}{1-\beta^*\cos\Theta_0} \qquad \Rightarrow \qquad \frac{\omega_{rad}}{\Omega_{rad}} = \frac{\lambda_u}{\lambda_{rad}} = \frac{1}{1-\beta^*\cos\Theta_0}. \tag{52}$$

The wavelength of the coherent undulator radiation emitted in the laboratory system under an angle Θ_0 becomes

$$\lambda_{rad} = \lambda_u\left(1-\beta^*\cos\Theta_0\right). \tag{53}$$

We replace now the average velocity β^* by the expression (39). Since the angle $\Theta_0 \approx 1/\gamma$ is very small, we can expand the cosine function in terms of Θ_0 as $\cos\Theta_0 \approx 1-\Theta_0^2/2$ and get the good approximation

$$\begin{aligned}\lambda_u\left(1-\beta^*\cos\Theta_0\right) &= \lambda_u\left[1-\left(1-\frac{1}{2\gamma^2}\left[1+\frac{K^2}{2}\right]\right)\cdot\left(1-\frac{\Theta_0^2}{2}\right)\right] \\ &= \lambda_u\left[1-\left(1-\frac{\Theta_0^2}{2}-\frac{1+K^2/2}{2\gamma^2}+\cdots\right)\right] \\ &\approx \lambda_u\left(\frac{\Theta_0^2}{2}+\frac{1+K^2/2}{2\gamma^2}\right).\end{aligned} \tag{54}$$

From this relation we finally get the very important ***coherence condition*** for the undulator radiation:

$$\boxed{\lambda_{rad} = \frac{\lambda_u}{2\gamma^2}\left(1+\frac{K^2}{2}+\gamma^2\Theta_0^2\right)} \tag{55}$$

For many experiments with synchrotron radiation the width of the spectrum lines emitted from an undulator is an important parameter. Because of the limited length of the magnet

$$L_u = N_u\lambda_u \tag{56}$$

the radiation has the time duration

$$T = N_u\frac{\lambda_{rad}}{c} \tag{57}$$

where N_u is the number of periods. In Fig. 14 the emitted wave pulse from an undulator is sketched.

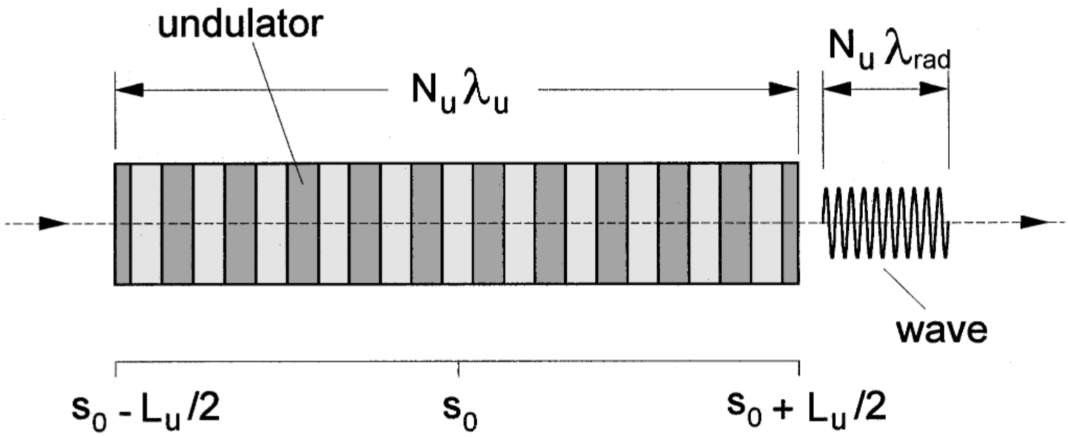

Fig. 14 Wave pulse emitted by a single electron passing through an undulator

The field strength of this undulator radiation can be expressed by

$$u(\omega_{rad},t)=\begin{cases} a\exp\left(i\,\omega_{rad}t\right) & \text{if} \quad -\dfrac{T}{2}\le t\le +\dfrac{T}{2} \\ 0 & \text{if} \quad \left|t\right|>\dfrac{T}{2} \end{cases}. \tag{58}$$

The resulting continuos spectrum follows from the *Fourier transformation* of the wave function:

$$\begin{aligned} A(\omega) &= \frac{1}{\sqrt{2\pi T}}\int_{-\infty}^{+\infty} u(\omega_{rad},t)\exp(-i\omega t)\,dt \\ &= \frac{a}{\sqrt{2\pi T}}\int_{-T/2}^{+T/2}\exp\left[-i\,(\omega-\omega_{rad})\,t\right]dt \\ &= \frac{2a}{\sqrt{2\pi T}}\,\frac{\sin(\omega-\omega_{rad})\dfrac{T}{2}}{\omega-\omega_{rad}}. \end{aligned} \tag{59}$$

With

$$\Delta\,\omega=\omega-\omega_{rad} \qquad \text{and} \qquad \omega_{rad}T=2\pi N_u \tag{60}$$

the amplitude of the partial wave is

$$A(\omega)=\frac{a}{\sqrt{2\pi}}\,\frac{\sin\left(\pi N_u\dfrac{\Delta\,\omega}{\omega_{rad}}\right)}{\pi N_u\dfrac{\Delta\,\omega}{\omega_{rad}}} \tag{61}$$

and the intensity (see Fig. 15)

$$I(\Delta\,\omega)\propto\left[\frac{\sin\left(\pi N_u\dfrac{\Delta\,\omega}{\omega_{rad}}\right)}{\pi N_u\dfrac{\Delta\,\omega}{\omega_{rad}}}\right]^2. \tag{62}$$

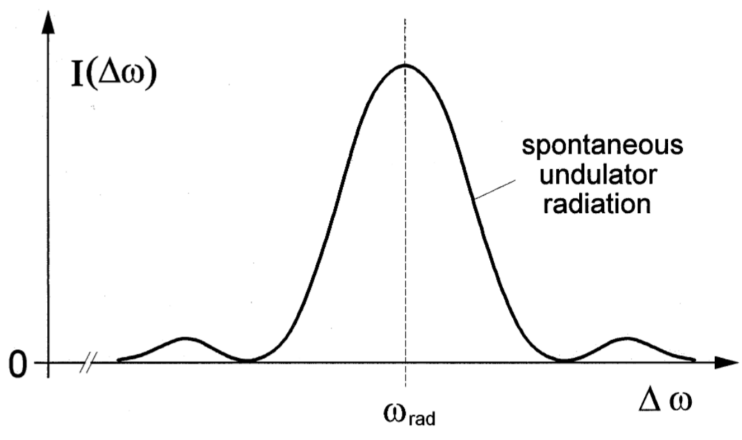

Fig. 15 Spectrum of the spontaneous undulator radiation

The full width half maximum (FWHM) of the spectral line can be found satisfying the condition

$$\left(\frac{\sin x}{x}\right) = \frac{1}{2} \qquad \text{with} \qquad x = \pi N_u \frac{\Delta\omega}{\omega_{rad}}. \tag{63}$$

The solution is $x = 1.392$ and we get

$$\frac{2\Delta\omega}{\omega_{rad}} = \frac{2x}{\pi N_u} = \frac{0.886}{N_u} \approx \frac{1}{N_u}. \tag{64}$$

The resolution of the undulator radiation is simply determined by the number of undulator periods. High resolution requires a sufficient large number N_u. Normally one can not observe these sharp spectral lines. There are higher harmonics and a frequency shift due to Doppler effect. A typical undulator spectrum is shown in Fig. 16.

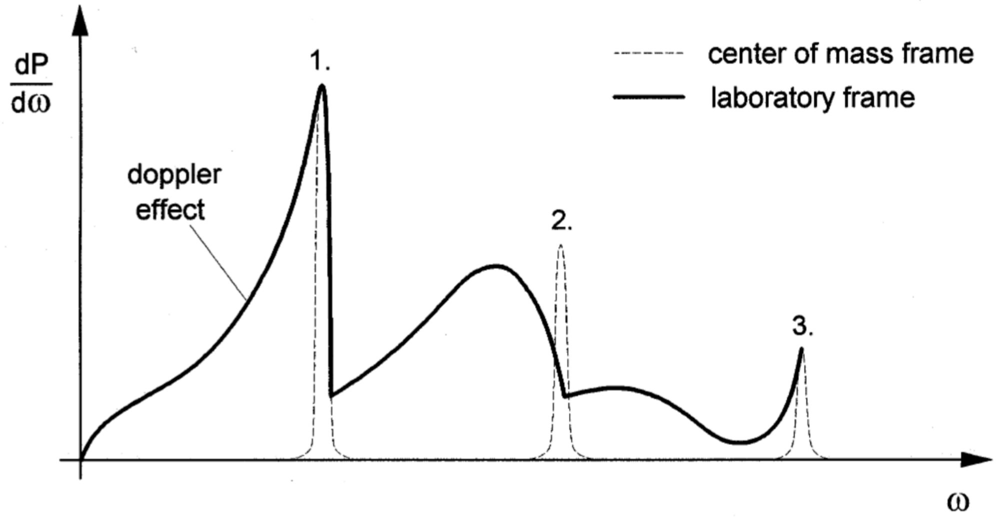

Fig. 16 A typical undulator spectrum

REFERENCES

[1] G. Brown, K. Halbach, J. Harris, H. Winick, Wiggler and Undulator Magnets - a Review, Nucl. Instr. & Meth. 208, 65-77, 1983

[2] H. Winick (editor), Synchrotron Radiation Sources - a Primer, World Scientific Publishing, 1994

[3] H. Winick, T. Knight (editor), Wiggler Magnets, Wiggler Workshop, SLAC, SSRP Report No. 77/05, 1977

[4] J. Spencer, H. Winick, Synchrotron Radiation Research, editor: H. Winick, S. Doniach, Plenum Press, New York, ch. 21, 1980